EUROPEAN SPALLATION SOURCE

MXType.Localized	
Document Number	MXName
Project Name	SKADI
Date	02/02/2017
Revision	MXRevision MXPrinted Version
State	MXCurrent

ESS Instrument Construction Proposal
SKADI

Small-K Advanced Diffractometer

	Name (name, title, e-mail address)	**Affiliation** (name of institution, address)
Proposer	Henrich Frielinghaus, Dr., h.frielinghaus@fz-juelich.de Sebastian Jaksch, Dr., s.jaksch@fz-juelich.de	Forschungszentrum Jülich GmbH, JCNS at Heinz Maier-Leibnitz Zentrum, Lichtenbergstrasse 1, D-85747 Garching Forschungszentrum Jülich GmbH, JCNS at Heinz Maier-Leibnitz Zentrum, Lichtenbergstrasse 1, D-85747 Garching
Co-proposers	Jacques Jestin, Dr., jacques.jestin@cea.fr Wim G. Bouwman, Dr., W.G.Bouwman@tudelft.nl	Laboratoire Léon Brillouin CEA/CNRS, CEA Saclay, 91191 Gif/Yvette Cedex, France Delft University of Technology, Mekelweg 15, 2629 JB Delft, The Netherlands
ESS coordinator	Andrew Jackson	ESS Lund

The following table is used to track the ESS internal distribution of the submitted proposal.

	Name
Document submitted to	Ken Andersen
Distribution	Dimitri Argyriou, Oliver Kirstein, Arno Hiess, Robert Connatser, Sindra Petersson Årsköld, Richard Hall-Wilton, Phillip Bentley, Iain Sutton, Thomas Gahl, relevant STAP

European Spallation Source ESS AB
Visiting address: ESS, Tunavägen 24
P.O. Box 176
SE-221 00 Lund
SWEDEN

www.esss.se

EXECUTIVE SUMMARY

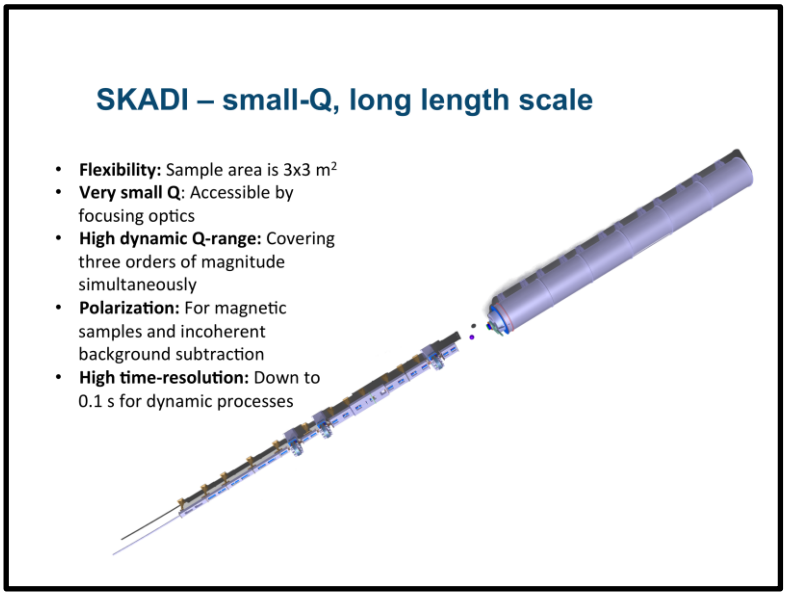

The **S**mall-**K** **A**dvanced **DI**ffractometer SKADI is a versatile SANS instrument, which enables scientists to perform a wide range of investigations on topics requiring small Q-values to access long length scales. The scientific areas targeted by SKADI include investigations of smart materials, biological and medical research, magnetic materials and materials for energy storage, as well as experiments on nanomaterials and nanocomposites or colloidal systems. These experiments promise a high potential impact on science and society. To maximize the societal applicability of these studies SKADI is designed to accommodate in-situ measurements with custom made sample environments to provide "real-world" conditions.

To achieve all these goals SKADI will feature the following general design properties:

- **Flexibility** (sample area is approx. 3x3 m^2, and versatile collimation)
- **Very small Q** accessible through VSANS (using focusing collimation elements)
- **Polarization** for magnetic samples and incoherent background subtraction
- **Good wavelength resolution**, being the longest SANS instrument
- **High dynamic Q-range** (covering three orders of magnitude simultaneously)

The first four of these features expands the science case into areas not covered by the LoKI and Compact SANS proposals. SKADI is envisaged as a vital part of the world leading SANS instrument suite for ESS, particularly in providing access to longer length scales and to polarized neutron measurements.

The 55 m long instrument allows for much space at the sample area and inside the collimation (last 12 m). It provides for simple access to bulky sample environment such as high field magnets or polarization analysis units, and also for large presses, load frames or other large deformation tools. Most of the topics that benefit from this feature lie in the hard matter field or involve magnetic particles. This large sample area also facilitates the inclusion

of custom-made sample environments. Additional in-situ setups for soft matter and biological investigations such as light scattering for an expansion of Q-space, rheometers, setups for strong electric or magnetic fields or shearing setups for directed self-assembly can be accommodated.

To be able to access the micrometer range in real space, as is needed for example in samples that exhibit a wide range of structural length scales, such as colloidal systems (colloidal aggregates and/or composites), it is necessary to be able to measure at very small Q-values. The versatile collimation allows for collimating elements that enlarge the achievable Q-range (VSANS option). This option will easily allow reaching 10^{-4} Å^{-1}, while we aim to reach a $5x10^{-5}$ Å^{-1}. VSANS will be realized by a series of converging collimation slits, to make use of the complete wavelength band while being insensitive to the effect of gravity on the neutron beam. This allows for a higher intensity than an equivalent pinhole arrangement. Due to the long instrument large slits are possible to minimize unwanted slit scattering and still achieve VSANS focusing. So VSANS and SKADI are ideally combined.

To be able to monitor this large Q-range in one measurement removes the need to repeat the measurement at another detector distance in the case of kinetic measurements. Even in the standard setup, without the VSANS option, SKADI covers a high dynamic Q-range of three orders of magnitude (typically from 10^{-3} to 1-2 Å^{-1}) and thus is excellently suited for such experiments. These include, but are not limited to, kinetic measurements on phase transitions in soft matter or biologic samples, which have gained increasing attention recently. This possibility to cover a wide Q-range in one measurement is also desirable where in-situ measurements cannot be properly replicated under the exact same conditions, for example increasing stress up to the breaking point of a sample.

Polarization of the incoming beam and polarization analysis after the sample enable full four-channel analysis of the magnetic structure. In this way, all magnetic structures can be identified clearly, opening up the opportunity for detailed analyses of magnetic materials with SKADI. Skyrmions are complex magnetic structures of much interest today, and SKADI is foreseen to analyze even more complicated magnetic structures and topologies. Another topic is magnetic nanoparticles, which are controlled by an external magnetic field. Here the possibility for polarization analysis together with the huge sample area to set up a magnetic field sample environment allow for a wide range of experiments.

While all SANS proposals make excellent use of the high brilliance of the ESS source, SKADI will make an ideal addition to the ESS SANS instrument suite because of its versatility allowing the investigation of a broad variety of samples under well-defined conditions. Intensity gains of 25 or more with respect to D22, one of the world-leading reactor based SANS instruments, are expected, because we make optimal use of the pulse length. With this high flux, SKADI allows for the investigation of fast kinetics (even for low scattering contrasts, where nowadays often model systems have to be used) and low concentrations of additives (or even traces). We expect that a time range of several tens of milliseconds will be achievable. Additionally, the long collimation allows for a very high Q-resolution. The wavelength band used on SKADI will be ideally suited for using polarizers, which generally only have a limited wavelength band in which they are feasible, thus no excessive intensity loss is expected for polarized scattering.

These features will allow SKADI to cater for the needs of a wide range of scientists, making it an ideal choice for a first day instrument. This is especially true in the light of the early success strategy by ESS, as SANS instruments have an excellent record of fast publication.

TABLE OF CONTENTS

Executive Summary 2
Table of Contents 4
1. Instrument Proposal 4
1.1 Scientific Case 4
1.2 Description of Instrument Concept and Performance 13
1.3 Technical Maturity 23
1.4 Costing 25
2. List of Abbreviations 27

1. INSTRUMENT PROPOSAL

1.1 Scientific Case

The advantage of SKADI lies in its ability to address a very broad science case, putting an emphasis on the flexibility of the sample environment, access to very small, precise polarization analysis and a high resolution in Q. These features will allow SKADI to widen the range of possible experiments in the overall ESS SANS suite, as these particular abilities are less pronounced in LoKI and the Compact SANS. This makes SKADI a good match as a day one instrument, as it will attract a wide range of researchers and combine this with the typically fast publication of SANS results. Given the growth in the number of fields employing SANS, the wider horizon of SKADI to enter new scientific areas will increase the demand further. The versatility of SKADI will enable it to address issues with a profound social impact that will have to be solved in the foreseeable future, among others topics such as energy storage, nuclear waste disposal and smart materials.

To cater for a wide range of different fields with an emphasis on in-situ investigations a wide range of custom-made sample environments is necessary. Some examples for such studies are: Shearing or electric and magnetic field setups to investigate induced ordering or directed self-assembly; rheometers to simultaneously investigate macroscopic mechanical and microscopic structural properties; load-frames and heating stages to investigate high temperatures in metal samples; and rigs for applying high mechanical strain.

1.1.1 Challenges for energy and environment

Energy consumption and storage as well as deploying environmental friendly techniques are among the most important challenges for science in the coming years. In order to address these challenges a number of key sample manipulation techniques are required. In particular, these include: high pressure (for the study of shale gas reservoirs[1] and gas storage [2, 3], especially hydrogen storage for mobile applications [4], CO_2 sequestration [5] and soil cleaning [6, 7], but also materials research [8] and other geological sciences [9]); uniaxial deformations (rubbers and other nanocomposites [10, 11], materials research and geological sciences [9]); and application of magnetic fields [12, 13]. The equipment for magnetism often involves large magnets with cryostats and polarization analysis. Also setups

for the simultaneous collection of non-neutron data, such as light scattering, spectroscopy or other yet to be deployed techniques are of importance in a wide range of fields. The versatility of the SKADI instrument with its large space for sample environment simplifies such studies.

Interest in the behavior of gases and fluids in porous media is increasing dramatically as a result of new techniques for exploiting energy resources, for reversible gas storage [2, 3] and for the sequestration of unwanted CO_2 [5]. In terms of energy storage for mobile applications, hydrogen storage plays an important role [4]. The length scales of the pores in materials of interest in these fields lie in the nanometer to micrometer range, and thus SANS and VSANS are ideal tools for such investigations. Elevated pressures can only be accessed in closed vessels, which makes investigation via the means of neutrons the method of choice. In this way, SKADI will help finding new solutions to today's problems.

The fluids used in soil cleaning (surfactant enhanced aquifer remediation) are aqueous surfactant systems [6, 16], which are fed in at the injection well and recovered at the extraction well, with the flow through the soil being pressure driven. The phase diagram and structure of surfactant micelles as a function of pressure and flow are often unknown. SKADI will allow contrast matched micelles to be studied in situ under pressure and in natural porous rocks or synthetic porous materials, where an excellent signal to noise ratio is needed to detect the small fractions of surfactant and the smallest amounts of polymer by selective deuteration (Fig. 1.1). In this way, the amount of surfactant used can be optimized with respect to functionality and ecological impact on the environment.

Materials are often tested under uniaxial pressures, tensions or shearing to probe macroscopic responses in combination with microscopic structural changes [10]. Composite materials of solids and soft compounds (often polymers) often provide the best mechanical performance [11]. The development of this field is still ongoing, and it is expected that SKADI will contribute to many new results. Car and truck tires are being improved to enhance energy saving performance, and hi-tech damping materials are being developed [17].

The response of natural rocks to pressure is of great interest for the stability of mines, for example to determine the feasibility as a radioactive waste repository [9]. The domains, the grain boundaries, and the cracks lie in the range of SANS, and study of these requires an extended Q range towards VSANS. Investigation of these structures over a wide range of length scales provides detailed understanding of the behavior of minerals in their natural

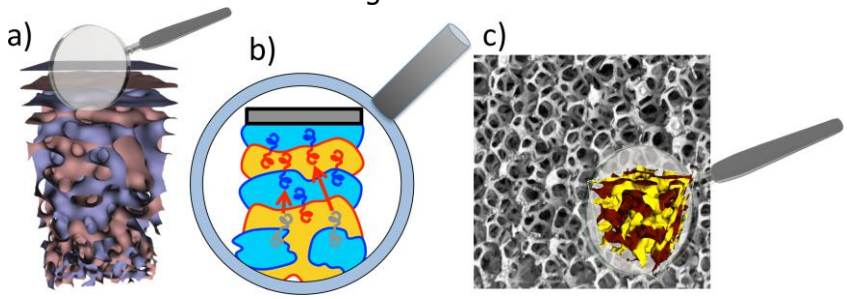

Fig 1.1. Microemulsions as model complex fluids (a) adjacent to planar walls [14], (b) with polymer additives that are attracted by the wall [15], and (c) in porous bulk media.

environment. Along the same line of thought, investigations of concrete to increase stability and durability are very important [18]. Here, as well as in natural rock, crack formation and plastic deformation are key mechanisms to be studied. Porosity studies have proved the applicability of the SANS method [19], and especially for natural rock the fractal nature of the sample makes a wide Q-range as offered by SKADI desirable. As previously mentioned, the use of neutron scattering makes the design of the sample pressure vessel simpler due to the penetrating power of the neutron beam. Furthermore, in this case huge sample equipment is necessary to achieve the necessary pressures. This is facilitated in the ample sample area for custom environments at SKADI.

1.1.2 Challenges for soft matter and biological studies

State of the art soft matter studies focus increasingly on functional soft/hard composite materials [20] and more especially on functional block entities for a better control of the self-assembly of 2D- or 3D-structures with either a designed response to external stimuli (smart materials) [21] or a controlled distribution of various species (like drugs or nutriments, metallic ions or nanoparticles) [22]. As these investigations are of basic relevance to modern medical research the impact on society of the results of this research could be immense. An inherent advantage of using neutrons in soft matter science is the possibility of contrast matching to improve the visibility of selected features in your sample [23], or even investigating mixing behavior which also requires a high flux to obtain high time-resolution [24] (see Fig. 1.2).

SKADI will be able to discriminate among various multi-scaled hard or soft structures (homogeneous, crystalline, cross-linked, meso-porous, fractal, aggregated, more or less organized) for which the interactions can be controlled chemically or physically. Examples for those stimuli, which make a precise and accurate control of the sample environment as in SKADI necessary, are pressure control [25] or temperature and light treatment [26].

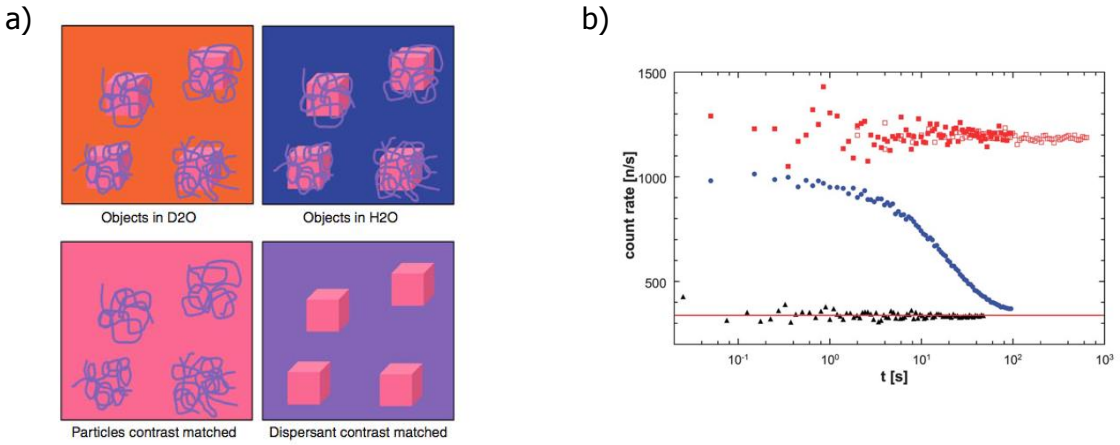

Fig. 1.2. A) Illustration of contrast matched particles in a solvent [23], b) Detector count rates as a function of time after mixing of purely deuterated and protonated micelles in a contrast matched solvent: C18– PEO5 (black), 50 ms time resolution; C24–PEO5 (blue) 100 ms time resolution; C30–PEO5 (red), 100 ms time resolution [24].

Monitoring these interactions by SANS and VSANS is also crucial in the investigation of the exchange or transfer through energy barriers (for example between engineered nano-materials and the membranes of living cells) with the goal of understanding the structure and dynamics of bio-interfaces at different length and time scales. Examples for this are self-assembled peptide [27] or carbon nanotubes [28] and DNA-origami [29]. Only by covering a wide Q-space will it become possible to connect transitions on different length scales in a sample. This will lead to a better understanding of the mechanisms governing self-organization and optimization of microstructures as found in nature.

The smaller scattering vectors in the Q-range of 10^{-4} $Å^{-1}$ are often needed in soft matter research when the structures are hierarchical. They can be purely synthetic (diesel fuel additives) [30] or appear in more natural bio-mimetic environments [31]. In order to reproduce application conditions as closely as possible, soft matter systems will involve mixtures of surfactants, polymers and solid colloids that are by themselves already different in size (see Fig. 1.3). The expected structures will have hierarchies that extend to µm length scales, again substantiating the need for the wide Q-range of SKADI. Applications are found in cosmetics, food and more technical applications (drilling fluid). Also colloidal samples may cover several orders of magnitude in their size distribution within one sample [23], for example as models for industrial paint. The understanding of the interplay between the different components and their specific tuning will enable even more medically compatible cosmetics [32], improved food recipes [33], and environmentally friendly chemical formulations [34].

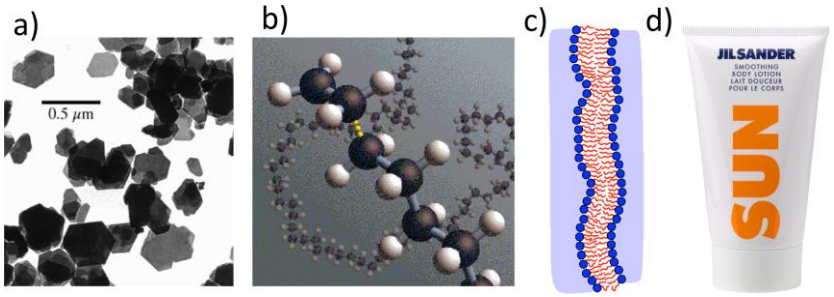

Fig 1.3. Many modern formulations contain (a) solid colloids, (b) polymers, and (c) surfactants or lipids that employ many length scales by themselves. Hierarchical structures are to be expected. One application is the sun lotion (d) or possibly paints.

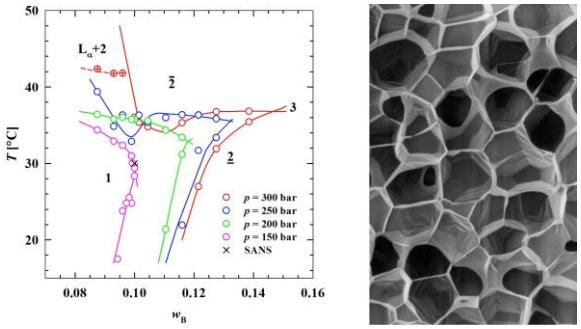

Fig 1.4. A phase diagram of a droplet microemulsions employing supercritical CO_2 at various pressures [35]. The temperature is plotted versus the water content. One aim of such formulations is the production of nano-foams (right).

Fast kinetic measurements are needed to study nano-foam formation where super critical CO_2 is usually expanded suddenly inside microemulsions of polymerizable liquids [35] (Fig. 1.4). This process happens only once, especially when the liquid is polymerized and cannot be reversed to its original state for repetition. Many length scales need to be covered simultaneously because the formed pores are usually polydisperse. SKADI will ideally allow for such investigations due to its large dynamic Q-range (three orders of magnitude) and the high intensities allowing short time slices, limited only by the mixing time within the sample containers (usually ~200 ms). These types of study will enable the development of nano-foams that provide the best performance in thermal isolation and low weight [36], and improve net zero energy houses.

1.1.3 Challenges for magnetism and hard condensed matter

As illustrated in Fig. 1.5, skyrmions are 'twists' of magnetic spins that cannot be smoothly deformed into another magnetic state i.e. they are topologically protected. The robust nature of these particle-like magnetic nanostructures bodes well for spintronic applications including information storage or logic devices [37], and motivates a rapid expansion of high-profile investigations [37-39]. Understanding how to control of the creation and motion of skyrmions is crucial [39], as are explorations to discover new materials that host skyrmions, particularly those with properties useful for applications [40]. As a quintessential probe of magnetic nanostructures within the bulk of materials, polarized SANS has already contributed greatly to the field [38, 41] and can be expected to play an important role in future explorations. As can be seen from Fig. 1.5, a reasonably high Q is sometimes required, together with neutron polarization analysis, which is useful for identifying the chiral symmetry-breaking nature of the skyrmion structure. The instrument setup of SKADI will permit rotation of the sample through the Bragg condition and support sample environment providing access to magnetic fields and to low temperatures.

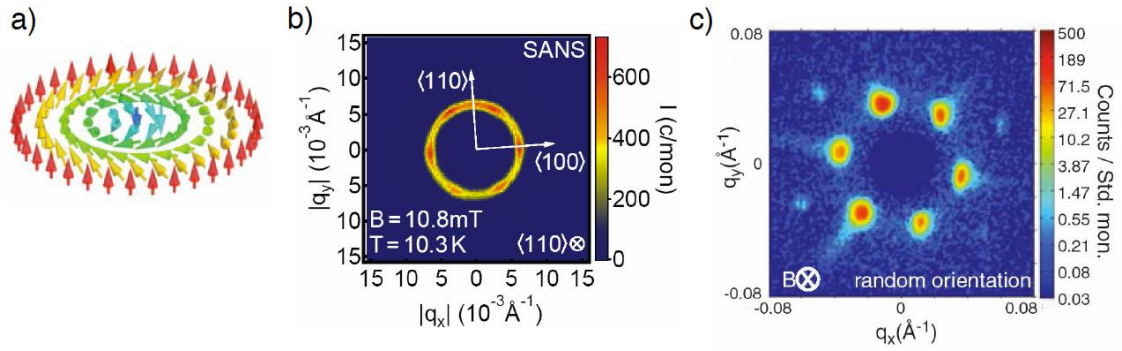

Figure 1.5. Probing skyrmion lattices with SANS. (a) Topological nature of a skyrmion. As one moves along a diameter, the magnetization rotates by 2 (from Ref. 28). (b, c) SANS images of skyrmion lattices in (b) $Fe_{0.5}Co_{0.5}Si$ from Ref. 30 and in (c) MnSi from Ref. 32.

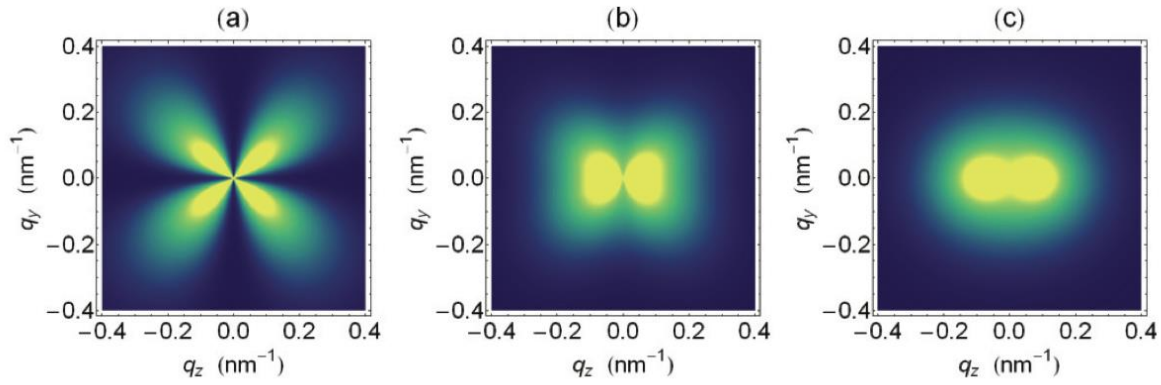

Fig. 1.6. Predicted scattering from magnetic nanoparticles in a nonmagnetic matrix at constant internal magnetic field of 2 T, with varying strength of the anisotropic field of a) 0.2, b) 1.6 and c) 8 in relation to the jump in field strength between nanoparticles and matrix [46]. Features such as these at low Q, which demand for a high resolution and polarization analysis, are an ideal application of the features of SKADI.

Magnetic nanoparticle systems are widely studied for their use in recording media [42], in permanent magnets and in biomedical applications including magnetic resonance imaging [43], induced hyperthermia [44], targeted drug delivery and cell activation [45].

Hyperthermia, for example, offers a route to cancer treatment with few side effects expected. Here magnetic nanoparticles at the cancer site are subjected to an alternating applied field, generating heat as their moments continually reorient to follow the field. In magnetic recording media, the goal is a film upon which many nanoparticles are assembled such that there are no interparticle interactions, with each nanoparticle presenting a blocked magnetic monodomain. There are also many promising applications for nanoparticle composite materials, e.g. for magnetic nanoparticles embedded in block copolymers [47, 48].

SANS is already a well-established tool for characterizing systems of magnetic nanoparticles [42, 49-52], and studies using polarized neutrons to separate the nuclear and magnetic components are common [49, 51]. With full analysis of the neutron polarization, it is even possible to resolve the local direction of the magnetization within the nanoparticle [50]. An example for the expected scattering from a two-phase magnetic system is shown in Fig. 1.6. These magnetic properties are only accessible for instruments with a delicate polarization analysis in combination with a high control of the sample environment as provided by SKADI.

Considering the growing potential and use of nanoparticles in applications, demand for polarized and unpolarized SANS beamtime will continue to rise. Further demand may also be expected for grazing incidence SANS (GISANS) geometries; this technique probes nanoparticles on the surfaces of films, and has recently been demonstrated with both unpolarized and polarized neutrons [48, 53]. Although SKADI is not designed to be a dedicated GISANS instrument, due to its long collimation it will be optimally suited to develop this capability at the ESS. As well as polarization analysis and GISANS setups, the SKADI instrument will be able to access the high Q needed for nanoparticle diameters ≤ 10 nm, and will support magnetic field and low-temperature sample environments. The high flux of the ESS will facilitate studies of the small nanoparticle yields, which are produced by the various

a) b)

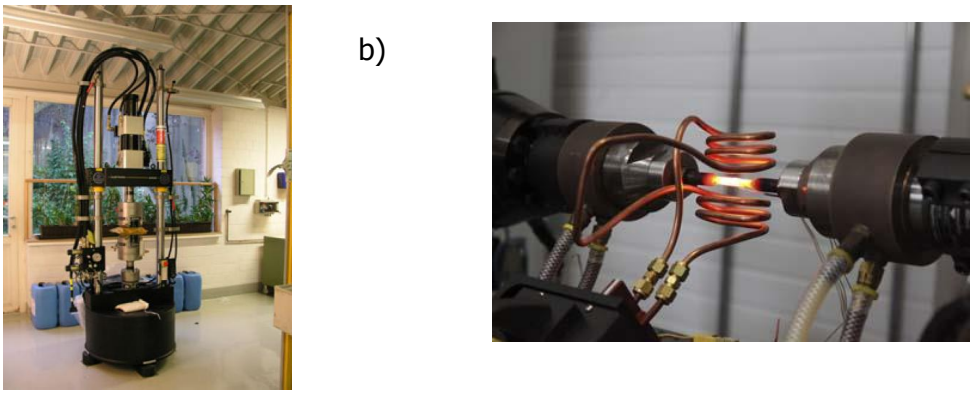

Fig. 1.7. a) Instron stress rig [55] and b) combined load frame with induction heating coil [56]. This bulky sample equipment requires a large sample area to set up and control sample conditions to achieve conditions as are required for application testing.

synthesis methods, even though the relative scattered intensity of these systems is too low for most of the state of the art SANS beamlines today.

In terms of polarization SKADI is excellently suited for this kind of experiment as most transmission polarizers only have a limited wavelength band for neutrons, which makes it difficult to use the complete pulse of a broadband spallation source in case of polarized scattering. In the standard setup, however, SKADI is designed to use a wavelength band of 2-7.5 Å, which is very suitable for cavity polarizers. Thus SKADI can operate in polarized mode without modification or excessive intensity loss.

Neutrons also are also indispensible when investigating samples under "real-world" conditions, which often requires thick or bulky samples, which could not be penetrated by x-rays. These investigations also often require extreme conditions, which can only be obtained with bulky equipment, such as load stress frames as a stress rig or a load frame induction heating setups (see Fig. 1.7). Setups such as this can be used to test equipment in-situ under stress or heating conditions, for example in testing turbine engine blades for aircrafts [54].

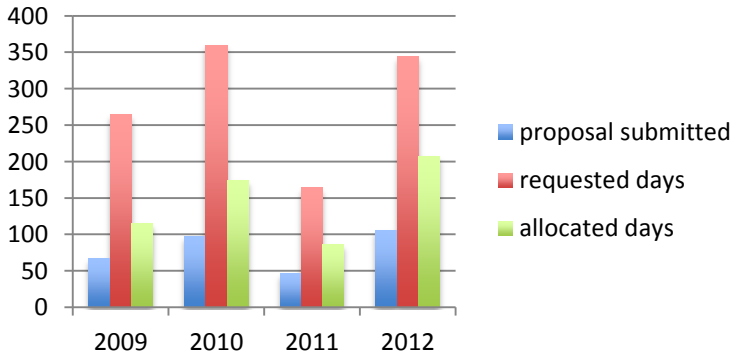

Fig. 1.8. Number of submitted proposals, requested and allocated beamtime at the SANS instruments (KWS 1/2/3) at MLZ. 2011 were less allocated days, due to a reactor shutdown.

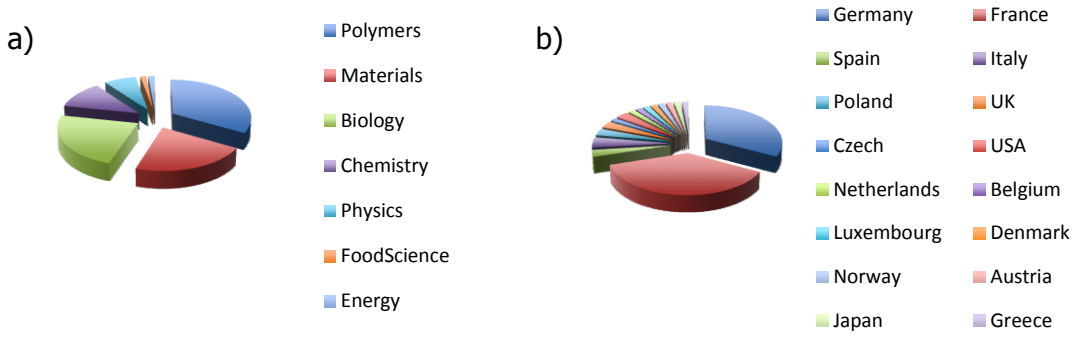

Fig. 1.9. a) Distribution of research areas of the received letters of interest for SKADI. b) Distribution of countries of the received letters of interest for SKADI.

1.1.4 User Base and Demand

The application of the SANS technique started in the fields of physics, chemistry, materials and soft matter science and has expanded to new fields such as biology, engineering, geosciences, energy and food science. The demand for SANS beamtime is constantly high, and so overbooking factors of 2 are common, while factors of 3 are also reached (see Fig. 1.8).

Even as new instruments have appeared, the demand remains high. Already, SKADI has attracted 70 letters of interest (see appendix) from European and international researchers. These are mainly in the traditional fields which usually perform SANS experiments, however there also is a user base in energy and food science, that shows great potential (see Fig. 1.9 a)). The user base is also well distributed over Europe with some international users (see Fig. 1.9 b)). By this we can see that there is an international demand for a world class SANS instrument.

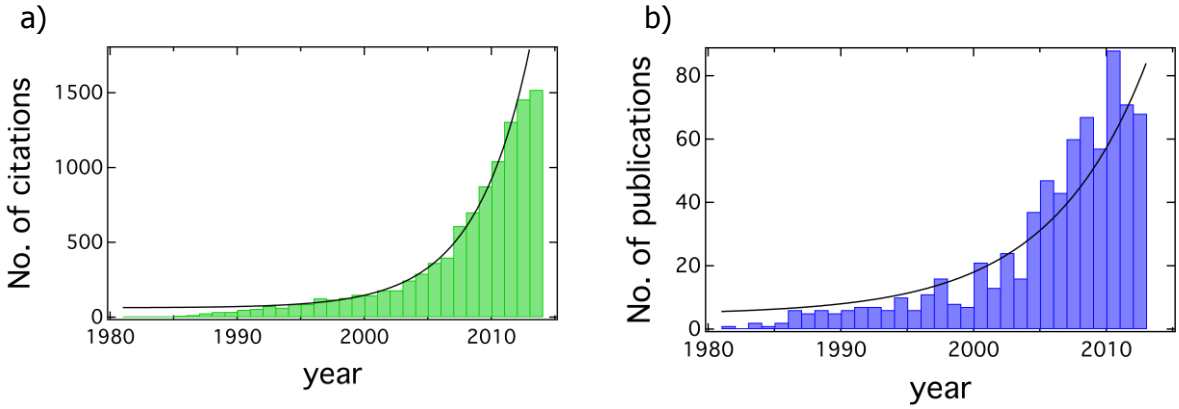

Fig. 1.10. a) Number of citations of SANS related research in biological studies, b) number of corresponding publications (raw data downloaded from www.isiknowledge.com).

The output of SANS instruments worldwide in the years 2000-2013 is roughly 700 papers annually (details in Fig. 1.11). All the major disciplines will find use for the SKADI instrument, with the hope of raising the demand in the less represented disciplines (SANS-wise). The high flux, the wide simultaneous Q-range, the polarization options and the low background will together with excellent possibilities for control of the sample environment open new perspectives for cutting edge research. Regarding the potential usage of the polarization we assume a demand roughly as for today's instruments which feature polarized scattering. This would account for 1/6th of the total beamtime to be used for experiments employing polarized scattering.

The disciplines, that are less represented today, will be attracted by the simple use (acquisition and data reduction) of the instrument in concert with well-developed sample environment. Here we expect a similar development as in the field of biological studies, which was also less represented in the 1980's (see Fig. 1.10). The future of SANS experiments lies in simplicity of experiment conduction so less experienced users become comfortable with the SANS technique. Thus, as yet unexplored possibilities for cutting edge experiments can be realized. While this is especially true for scientific areas which do as of yet not have a high representation in the SANS area, also the traditional fields will strongly benefit from these improvements.

In the light of the early success strategy adopted by the ESS, SANS instruments in general show a great record in terms of fast and high quality publication. Once the ESS is fully operational in 2025, it is expected that SKADI will serve for 120 experiments per year with a similar high publication output.

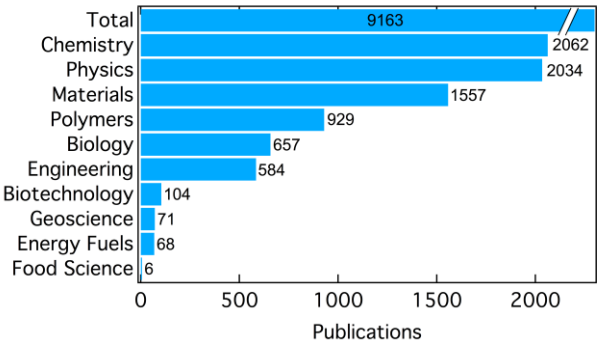

Figure 1.11. Statistics about SANS publications in the years 2000-2013 sorted by topics. It will be a task of SKADI to support the less well-presented topics in the near future.

1.2 Description of Instrument Concept and Performance

The general aim of this SANS concept is to design a versatile instrument, reaching to lowest possible Q with a high Q resolution and providing the possibility for polarization and extensive focusing optics. The classical sample size (1x1 cm^2) allows for highest scattering intensities whilst still enabling many kinetic experiments, for example in stopped-flow cells. In this way, very small time slices will be possible in kinetic experiments, in most cases easily down to the mixing limit of up-to-date stopped flow cells. In the case of non-kinetic experiments, fast measurements are highly desirable to test a maximum of conditions in a given experimental time. In particular the scientific output of many experiments lies in the variation of parameters that reveal the central mechanism in the system being studied.

We propose a rather long instrument with a collimation of 20 m and a detector tube of 20 m (see Fig 1.12). In such long instruments the implementation of neutron polarization does not affect the underlying concept, as there are multiple possible locations for a polarizer. This serves to enhance the versatility of the instrument. One can study many materials with magnetic domains or flux lines, and separate coherent and incoherent background. The extra space obtained by having the sample position further from the moderator allows for large magnets or other custom sample environments (cryostats, load frames, high temperature stages), and polarization analysis (preferentially with ^{3}He). This allowance for a huge variety of possible sample environments is an indispensible feature of modern SANS instruments. The separation of incoherent background is highly desirable for weakly scattering samples with important details at larger Q, especially so for biological molecules and complexes.

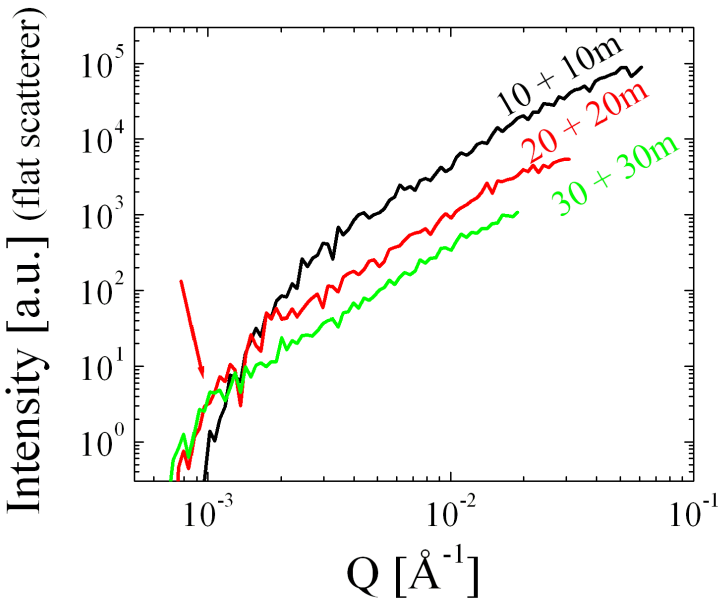

Fig. 1.12. Comparison between different collimation and sample detector distances. The 20+20 m option is clearly favorable at low Q, as compared by a flat scatterer. The 30+30 m option only shows little gain over this option, while the 10+10 m option already is at much lower intensity.

The central goal for the proposed SANS concept is a wide Q-range with the maximum intensity possible for the smallest Q, because for good statistics the experimental counting times mainly depend on the lowest count rate at any given Q in the Q-range. The condition of a wide Q-range usually favors rather short instruments, because here a wide bandwidth of wavelengths can be used. At fixed detector geometries, the shorter instruments serve for smaller Q, as they can employ the widest possible wavelength band. In contrast, the neutron spectrum of the cold source provides the highest intensities at short wavelengths, which usually favors large Q. The underlying concept of this instrument is to employ relatively small wavelengths with high intensities for the small Q by means of a high detector resolution as well as constructing the whole instrument with a relatively large length of 9.5+20+20 m (for bender and polarizer/ collimation/detector tube). This concept renders homogenous intensities and therefore comparable statistics for the small and the high Q area. Thus counting times for both Q areas are in the same time regime.

Another favorable feature of the long instrument is the good wavelength resolution. Here, the spread of the wavelength band is naturally high, and the different wavelengths are much better separated. The different time slices at the detector position allow for wavelength uncertainties of typically 4 to 8%, and can be even reduced to ca. 2% when choosing only large wavelengths.

1.2.1 Instrument Overview

SKADI has a maximum sample-to-detector distance of 20 m and a maximum collimation length of 20 m. This provides for the highest intensities at the low Q end and for balanced statistics over the whole Q-range. Including the beam preparation of 9.5 m the overall instrument length is 50 m (+2 m for moving detector tank), measured from the source to the end of the detector tank. Figure 1.13 shows the layout of the instrument.

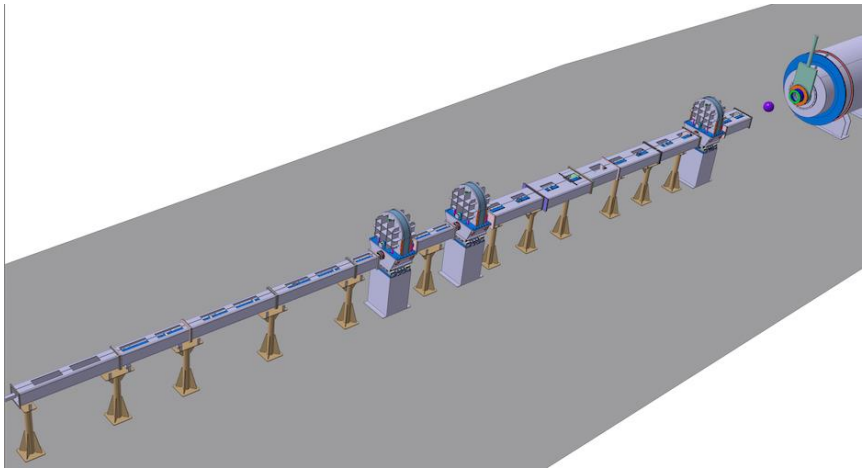

Figure 1.13. Layout of SKADI after the beam preparation. For clarity only the entrance of the detector tube is shown and shielding is omitted. From left to right: Slim and wide collimation with choppers at 11.5, 14.5 and 21.5 m, sample position (lilac sphere) and entrance to the detector tube.

There are two primary modes of operation for the pinhole SANS: (1) aiming for maximum flux and so every pulse is used. The wavelength bandwidth is then 5.5 Å while the actual range can still be chosen as 2-7.5, 4-9.5, or 10-15.5 Å for example. (2) The bandwidth can be doubled by skipping each second pulse, and so bands of 2-13, 4-15 Å can be selected. Typical minimal Q lie in the range of 0.5 to $1x10^{-3}$ $Å^{-1}$, and maximal Q in the range of 1 to 2 $Å^{-1}$ depending on the settings. Additionally, at shorter collimation length in order to maximize neutron flux at the sample, a SDD of 8m can be chosen, allowing for wavelength bands of 7.2 Å.

The cold source is designed by the ESS (in terms of simulations and in reality) and operates at ca. 20 K. At the shortest distance of 2 m, the bender is placed with a length of 4 m. Then, a polarizer with radio frequency spin flipper will follow. After this, the collimation of 20 m length is placed. The first 8 m will be narrow for reasons of angular space between different instruments. After that, the last 12 m will have a wider housing for more equipment. Currently, focusing slits for VSANS and a SESANS option are under consideration to allow for larger length scales (down to ca. $5x10^{-4}$ and several 10^{-6} $Å^{-1}$). The evacuated detector tube will host two 1 m^2 area detectors, the first one of which has a central 20x20 cm^2 aperture. Furthermore, detectors with very high resolution are under consideration for primary beam detection, the VSANS (3x3 mm^2), and the SESANS (55x55 μm^2) option.

Independent of this, the broader collimation housing at the last 12 m in front of the sample allows for focusing optics that extend the minimal Q to ca. $0.5x10^{-4}$ $Å^{-1}$. This option replaces the classical collimation and, therefore, requires separate acquisition. The SESANS option discussed by Delft would allow for simultaneous counting of classical SANS spectra and SESANS scattering (Q-range ca. several 10^{-6} to 10^{-4} $Å^{-1}$, but leaving the gap to classical SANS). Both very low Q techniques require a high-resolution detector in the beam center: Focusing SANS a 25x25 cm^2 detector, SESANS a 7x7 cm^2 detector.

1.2.2 Beam Delivery

The whole guide concept is based on neutron guides of 3x3 cm^2 cross-section and the typical coating of m=1.0.

Bender

The task of the bender is to avoid the direct line-of-sight for the scattering experiment. At this point, a reference design provided by Andrew Jackson from the ESS is used. This is to ensure comparability during the evaluation process. The reference design features a 3x3 cm^2 cross section. It is bent at a radius of 78 m over a total length of 4 m and lined with m=4 material. To ensure high transmission it is a 4-channel bender.

During the initial engineering phase of the construction project alternative designs will be considered, and optimized to the specific needs of SKADI. In this regard this we are already evaluating single and S-bender geometries that allow for a maximum transmission at low divergences. We are also looking into the possibilities of channeled benders as well as asymmetric benders with different aspect ratios of the cross section.

Wavelength Band Selection

The wavelength band used in a SANS experiment will be selected by a set of three choppers placed at 11.5, 14.5, and 21.5 m from the source. Two co-rotating discs will allow for

variable opening times, which is needed for the wide wavelength band mode. The choppers fit in the gaps of the 1m sections of the collimation.

Two different modes for the standard operation are envisaged: The high intensity mode chooses the band between 2 and 7.5 Å, while the wide Q-range mode skips every second pulse and allows for a band between 2 and 13 Å. The first mode is optimized for experiments that explicitly know the interesting Q-range and highest intensities are the priority. The other mode will be used for experiments with less well predictable Q-range (beforehand), and so the maximum dynamic range is the main purpose. Especially, kinetic measurements with growing objects are such an example where the length scales cannot be predicted beforehand.

The flexibility of the chopper settings will allow for any wavelength bands that are reasonable. So, it might be preferential to skip the lowest wavelengths, and focus on a band of 4 to 9.5 Å for more classical SANS samples. Apart from this, for focusing on the lowest scattering vectors Q a range of 12 to 17.5 Å might be useful. Furthermore, a smaller maximum detector distance of 8m would consequently enlarge the usable bandwidth at 14 Hz from $\Delta\lambda$ = 5.5 Å to $\Delta\lambda$ = 7.2 Å.

Prompt Pulse

Inadequate blocking of fast neutrons and other radiation might cause an unwanted background that had not been blocked by the bender and the choppers. This topic is one of general relevance to all instruments at ESS and must be addressed as part of the risk management (section 1.3.2). Minimization of this background is especially needed when the long wavelengths, with their naturally low intensities, are important for the experiment.

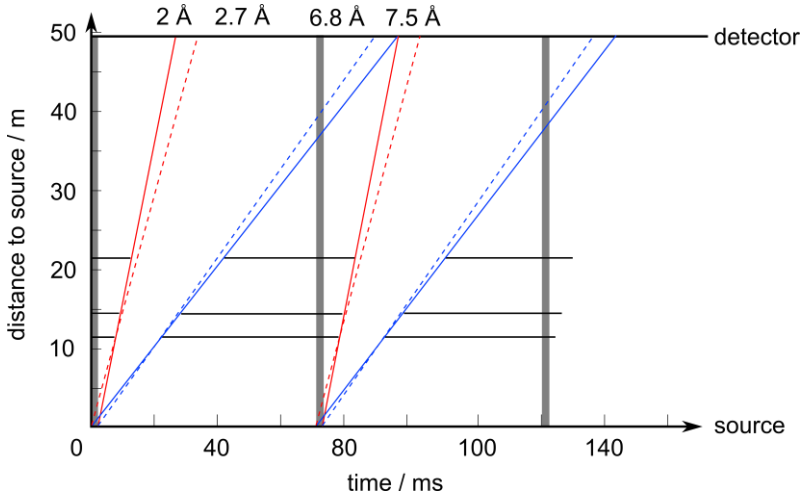

Fig. 1.14. Time-of-flight diagram for SKADI at a 20 m detector setting with a usable wavelength band between 2 and 7.5 Å. The choppers are placed at 11.5, 14.5 and 21.5 m from the source. The intensity will ramp for the initial 2 to 2.7 Å and the higher 6.8 to 7.5 Å neutrons due to the chopping.

Chopper Speed

The chopper speed in the normal modes 1 and 2 is 14 and 7 Hz (840 and 420 rpm). The transition times for opening and shutting the beam might be a problem. We propose choppers of 60 cm diameter with two co-rotating discs. The typical shutting times are then 0.9 and 1.8 ms. If we allow the transition regions of the first and last time frame to overlap, and agree on rejecting these data, then still the central time frames will carry the major intensity. This rejection will be removing low intensities in any case.

Polarizers / Analyzers

Two polarizers will be made of two cavities each. Each cavity will host a V-shaped supermirror that is optimized for a certain wavelength band. The resulting wavelength bands are 4 to 12 Å and 12 to 20 Å. A vertical changer will exchange between them and a plain guide for non-polarized neutrons with double intensity. Such a polarizer has been installed and commissioned on KWS1 at MLZ. For analyzers we propose ^{3}He SEOP cells that are optimized for either small or large angles. Experience exists for the beam lines MARIA and KWS1 at MLZ. Limited wavelength bands are not an issue with SKADI, since the default wavelength band is $\Delta\lambda$ = 5.5 Å.

Guides and Collimation

All linear guides will carry an m-value of 1.0, which allows for a minimal collimation of 4 m with the full divergence at a wavelength of 2 Å. This mode might be rarely chosen, but for finely sliced real time measurements one might chose this mode in order to resolve fastest kinetics in the range of around 100 ms. The longer collimations of 8 m and 20 m will require good absorption of superfluous neutrons whilst maintaining a low gamma background.

The collimation itself consists of movable 1m neutron guides between 4 m and 20 m (from the sample) allow for adjusting the entrance aperture distance in 1m steps. Variable diaphragms at fixed distances of 4, 8, 14, and 20 m will allow for fine-tuning the exact aperture cross-section and shape. On top, the rectangular apertures might be used for the GISANS option where slits are the ideal shape.

At a distance of 1 m there will be further absorbers of 3x3 cm^2 if the corresponding neutron guides are moved out. These passive apertures will simply absorb highly divergent neutrons that are not caught by the defining apertures. The collimation as described so far will extend over the distance of 4 to 20 m. On the last 12 m (to the sample) we intend to allow for a wider changer with more choices of possible optics and/or magnetic guide fields. The high-resolution option with converging slits will drive the minimum Q down to 5x10^{-5} Å^{-1}. The SESANS option will need magnetic guide fields and flippers around and in the beam. Both options are best implemented in the last 12 m since much longer versions of the two techniques have not been proven to be feasible, and the angular space used by the instrument should be kept reasonably low.

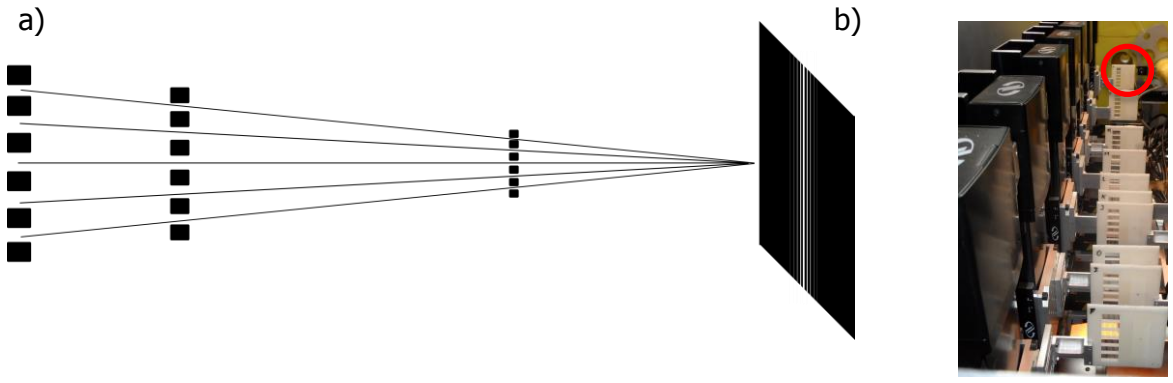

Fig. 1.15. a) Top view sketch of the vertical slit system for VSANS optics. N masks made of several diaphragms with slits whose number and positions focus the neutrons on the detector plane. b) Image of the focusing setup at the TPA at LLB, France, illustrating the slit masks arranged along the collimation (3 m) using 9 diaphragms. Sample position is marked by a red circle.

1.2.3 Optional Instrument Optics

VSANS

The VSANS method aims at ca. 10 times smaller scattering angles than the classical SANS method [57]. To achieve this, the primary beam must be 10 times smaller (so ca. 3x3 mm^2) on the detector using focusing methods. There are focusing mirrors and lenses that replicate the small entrance aperture on the detector 1:1. Here, the proposed VSANS technique uses multiple converging slits or apertures for the same purpose, beginning with the original cross section of the neutron guide for the complete set of apertures. The sample is always placed at a position where the whole incoming neutron field is still relatively wide (either after the mirror/lenses or in the middle of the first aperture and the detector), and so larger samples are needed for this intensity demanding experiment. Here, for the proposed method, the typical sample size will be 1.5x1.5 cm^2, and thus not much bigger than for classical SANS. The only disadvantage of the proposed method is the influence of gravity that would result in a wavelength selection in the case of apertures or horizontal slits. Vertical slits would allow for enough flexibility that no wavelength selection takes place. The horizontal slits are nonetheless still in discussion for the combined GISANS/VSANS option when the vertical divergence must be well defined (see next section).

The VSANS option will be a focusing multi-slit converging beam collimation that could be operated or removed according to the user's needs. The multi-slit concept is a series of N masks made of several slits (typically of 1 mm aperture) that reduce the beam size and focus the neutron on the detector (Fig. 1.12a). The number of masks, their respective positions as well as the number and the size of the slits will be determined by McStas simulations. In order to be insensitive to gravitational effects, vertical slits will be used. The total length of the multi-slit collimation system will be between 1 and 3 m and will be located in the front part of the collimator just before the sample position. The expected Q range, between $\sim 10^{-4}$ and 10^{-2} $Å^{-1}$, will allow significant extension of the classical SANS Q domain, 10^{-3} to 1 $Å^{-1}$, with a good overlap while maintaining a good spatial resolution.

A feasibility study is currently performed at the LLB with a combination of simulations and real multi-slits TOF experiments on the operating VSANS spectrometer (see Fig. 1.15). Alternative approaches for reaching low Q down to 10^{-4} $Å^{-1}$ are discussed in the risk section.

GISANS

In order to be able to probe surface structures on substrates, a grazing incidence SANS setup can be realized with little additional effort on SKADI as the essential components, such as a good collimation and high-resolution detector, are already in place. Two horizontal slits that are shaped by the classical rectangular apertures in the collimation will allow for performing experiments with inclining/declining incident angles of up to ±0.2° for a horizontal sample position (the critical angle of D_2O vs. air is around 0.5°, and will not be served without declining collimation, that is currently not considered), while vertically the sample will always be turned by the sample stage. The classical Q range will be on the same order of magnitude as for SKADI without VSANS option (while the combination is still under discussion). McStas simulations will be used to determine an appropriate slit size and position for the desired Q-range and depth resolution, and typical intensities to be expected.

SESANS

The SESANS technique aims at even smaller Q, or larger length scales, than VSANS. Typically, several 10 µm can be achieved. Technically, the neutron spin is used to encode the different extremely small scattering angles [58]. As for all spin-echo methods, a Fourier transformation takes place that in the case of SESANS delivers the real-space correlation function. Since the scattering angles are extremely small, a high resolution detector is needed at the place of the beam stop (preferentially with 100 µm resolution), while for the classical SANS angles the scattering intensity can be detected in parallel serving for an extremely wide Q-range simultaneously.

The SESANS option ideally suits to the SKADI instrument for reasons of space in the collimation section. The SESANS option will allow for largest length scales to be measured in the range of several 10 µm. This option is an independent Dutch in-kind project based at the Reactor Instituut Delft and will be evaluated separately at a later time.

1.2.4 Sample Area

The default sample area will extend by 1 m towards the source and a few ten cm towards the detector. From the collimation side, a movable nose will make sure that the vacuum guide extents maximally towards the sample. The detector tube shall provide a relatively large window for largest scattering angles. For huge sample environments, it might be needed to move the detector tube backwards. We propose a motor driven 2 m rail system for the whole detector tank. An encoder must be used to determine the real detector position from the tube movement and the inside detector movement to a precision of a few mm. In this way a space of 3 m is achieved in the flight direction. In this way a perpendicular space of 3 m could be achieved for the sample position, resulting in a maximal space of 9 m^2 for custom sample environment.

The suite of sample environments for SKADI will contain changers (be it distinct cells or injection changers), typical soft-matter environments (rheometers, Peltier ovens, high

precision temperature ovens), high precision positioning systems (hexapod), magnets (1.5 T, 5 T, and highest possible field), and a variety of cryostats and high temperature ovens. For mechanical load experiments stress frames as well as other mechanical load setups are conceivable. Usually, the more expensive apparatuses will be shared between different instruments.

1.2.5 Detectors

The general setup of the detectors is planned to be a two-stage system with a first detector at 0.2 of the collimation length and a second one at the full collimation length. The first one will have a 20x20 cm^2 aperture at low angles to allow neutrons to the second detector for the low Q-range. By virtue of higher distance and better angular resolution the detector at the far end will give a higher Q resolution. Moreover by covering a wide Q range simultaneously this setup accommodates real-time measurements, especially single-shot measurements. The slight angular gap between the two detectors will not result in a gap in Q space due to the TOF capability of the instrument.

We discussed different options concerning the neutron detection technology with the ESS detector group (Kalliopi Kanaki, Richard Hall-Wilton).

To achieve these goals and at the same time have a reliable technology in terms of engineering feasibility and endurance we propose a system made up from modular photomultipliers. In combination with a ^{6}Li scintillation converter these would allow for count rates in the GHz range over the whole detector, at this point presumably only limited by the counting electronics. The pixel resolution of these detectors is 6.125 mm in both directions, thus there is no need for the Auger approach to improve resolution. New detectors with a pixel resolution of 3x3 mm^2 are already available, so we propose to use them for the zero-angle detector. Here we will use the highest resolution available at the point of purchase, as substantial improve to values as low as 1.5x1.5 mm^2 are expected within the next years. Possibly they will have to be protected by an attenuator, however this will allow for the measurement of the complete scattering image without impediment by a beam stop. As photomultipliers of these types are already commercially available we do not expect problems during the engineering phase and have requested a prototype for the end of 2014. Detector alternatives are detailed in the risk section.

1.2.6 Estimates of Instrument Performance

Q-range and Resolution

The resolution of a SANS experiment is determined by uncertainties of the wavelength and the direction of the beam. The latter is tightly connected to the divergence, determined by the entrance and sample aperture. The spatial detector resolution appears as a fourth term. While the resolution function for classical reactor source SANS is well known theoretically and experimentally, the experimental implications for time-of-flight SANS instruments are currently explored at several instruments around the world. Mainly, the wavelength spread is tightly connected to the 3 ms pulse duration. It weighs stronger for the short wavelengths and becomes exceptionally low for large wavelengths. The geometrical resolution stays conventional.

The resolution can be addressed best using computer simulations with a sample that produces sharp Debye-Scherrer rings. An example is plotted in Fig. 1.16. The original delta

peaks are three per decade in Q. The relative width of the peaks (δQ/Q) increases to smaller Q where, as usual for SANS, the geometrical resolution worsens as it is dominated by the detector pixel size and pinhole collimation aperture sizes. Such simulations were used for the benchmarking of SKADI (see next section).

The obtained Q-range for the 8 m experiment (and 1.6 m second detector and wide wavelength band) is between 1.3×10^{-3} to 1.5 $Å^{-1}$ (Fig. 1.16). Additionally a setup with 20 m SDD is evaluated (Fig. 1.17). The simulations do not deal with the noise, especially important for lowest intensities at smallest Q and largest Q (limited bins at detector edges and wavelength band limits). Nonetheless, we are optimistic to cover a dynamical Q-range of three orders of magnitude in a single shot. For the 20 m detector setting, the Q-range is slightly reduced, but still the simulations suggest a dynamic range of three orders of magnitude.

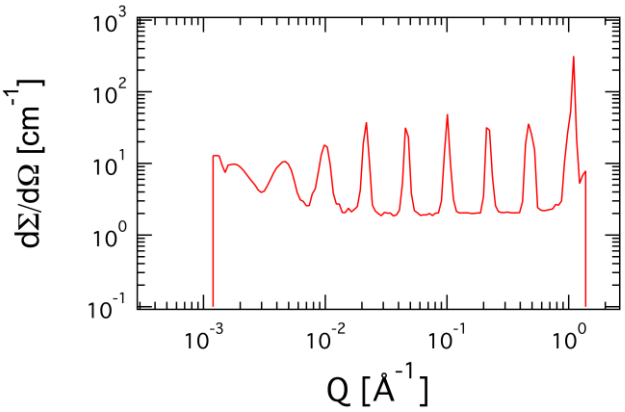

Fig. 1.16. The resolution simulation experiment for SKADI calculated back to absolute intensities. The detectors are placed at 8 m and 1.6 m. The used wavelength band was 2 to 15 Å without choppers (simulated skipping every 2nd pulse). Only a single pulse was simulated, so there is no overlap of slow and fast neutrons from consecutive pulses.

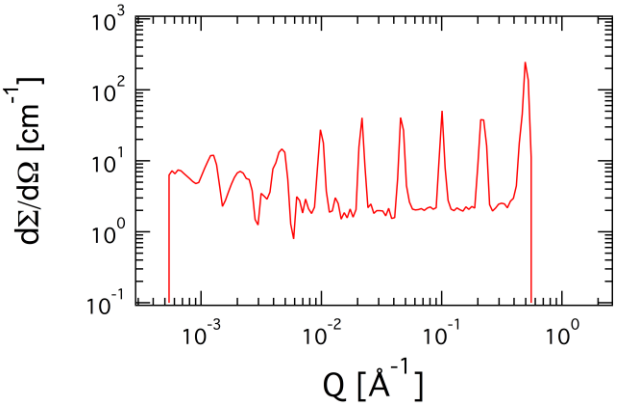

Fig. 1.17. The resolution simulation experiment for SKADI calculated back to absolute intensities. The detectors are placed at 20 m and 4 m. The used wavelength band was 2 to 13 Å under the same conditions as in Fig. 1.13.

Neutron Beam Intensity

The intensity of SKADI is compared to D22 using a water sample and 8 m detector distance (Fig. 1.18). The intensities are given in units of cps and grow with a Q^1 power law. The reason is the growing circumference on the detector at constant Q, and the Q-binning on logarithmic scales. For D22 we also assumed two simultaneous detectors at 8 and 1.6 m distance. The pure intensity comparisons result in gains of 20 and 29 for SKADI versus D22 depending on the wavelength band in use (2 to 9.2 or 4 to 11.2 Å) and the choice of the detector position at D22 (see fig. 1.18).

For the Figure of merit (FOM) we developed another formula based on an ensemble of infinitely sharp Debye-Scherrer rings. While the original formula was developed for single Bragg peaks, the ensemble allows for spanning the whole Q-range with information. This situation is closer to the experimental conditions where features are spread over several positions in Q-space. The new FOM reads now:

$$\mathrm{FOM} = \sum \frac{I_{\mathrm{peak}}}{s_Q(Q)}$$

This formula we applied to the bare count rates of the multiple Debye-Scherrer rings. The widths of the peaks σ_Q was analyzed individually; and the peak intensity I_{Peak} read off at the maximum. The comparison between D22 and SKADI resulted in a gain of the FOM by a factor of 35.8 and is quite independent of the exact settings of the instrument. This especially supports this concept of the FOM.

The underlying difference of the pure intensity gain and the FOM results from the weaker resolution of the time-of-flight instrument that always includes the short wavelengths.

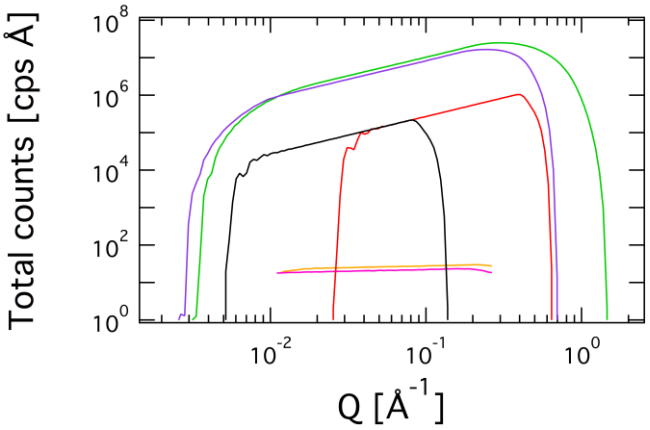

Fig. 1.18. Intensities of 1 mm water sample (1x1 cm^2) for instruments SKADI (green, lilac) and D22 (black, red). The divergence was identical (SKADI: 3x3 cm^2 diaphragm at 4.8 m collimation and D22: 4x5.5 cm^2 at 8 m). The detectors were placed at 8 (black) and 1.6 m (red). For SKADI the wavelength bands of 2 to 9.2 Å (green) and 4 to 11.2Å (lilac) were chosen. The pure intensity ratios are between 20 and 29 at each given Q value.

1.3 Technical Maturity

This part focuses on the components needed for a time-of-flight SANS. In particular the mechanical and optical components do not demand new technologies and are readily available. In contrast, the detector for SKADI at the ESS should be able to count more than 20 MHz – at least this would be the optimum requirement. So far, this has not been developed but we have presented a feasible approach to resolve this issue.

1.3.1 Location

The whole instrument is designed to fit in the angular space that is foreseen for all the instruments. The near source components are kept slim, and the collimation becomes wider at a distance of ca. 17.5 m. So the minimum demand does not stress the common conditions for all instruments.

Since the sample environment would allow for much space in the neutron direction and perpendicular, it would be ideal to give SKADI an outside edge position, such that heavy magnets, cryostats and other large sample environments would be installed from the side and not only from the top by using a crane. We would like to give the detector tube a rail system from the outside to be able to move the tube back by 2 m. Mechanics and measurement systems are available that will be able to determine the detector positions exactly down to 1-3 mm which is needed for the exact time-of-flight paths.

1.3.2 Risk Management

Shielding

Most of the shielding will be constructed from concrete. The angular space will allow for thick enough walls; only at the near bunker position the shielding between different instruments might get thinner. The main access point will be at the sample position, and so the shielding must be safe for free access for sample environment installation and sample changes. Apart from that there must be movable doors for closing the sample environment during the experiment.

The direct line-of-sight needs to be shielded well for high signal-to-noise ratios. The chopper absorbers need to work well for unwanted fast neutrons.

In the other facilities operated by us (KWS 1, KWS 2 and KWS 3 at MLZ, FRM2) we gained sufficient experience to reasonably layout the shielding, based on conservative estimations. Furthermore, there will be support from ESS.

Beam Delivery System

Most of the neutron guides are classical components. Most of the neutron guide providers are delivering these m-values within their standard procedures.

VSANS

As alternatives we are evaluating MgF_2 lens systems, which would focus primarily the long wavelengths needed to achieve low Q. Another fall back option is the usage of a toroidal

mirror, a system currently used at the KWS 3 at MLZ, FRM2. Here the advantage is the whole wavelength band can be focused simultaneously.

Detectors

For the detectors we consider many different solutions in parallel. Generally, two demands for detectors have to be distinguished: The primary beam detector needs to deal with the extremely intense beam. A good resolution would be beneficial for the center determination and for the VSANS and SESANS options. The two large area detectors (1 m^2) need to deal with lower, but still high, intensities (ca. 20 MHz) and the spatial resolution can be relaxed to 5 to 10 mm.

The LLB has good expertise in ^{3}He detectors. Here, parallel tubes allow for high counting rates of ca. 5 MHz (experience of today, maybe 20 MHz). Increases might be achieved by extending the array in the neutron flight direction with thinner tubes or by putting several tubes with lower He-pressure behind each other. The tube diameters still need to be determined, but an overall active area of 1 m^2 is the aim. The suppression of gamma background is most easy with ^{3}He detectors, and usually the distribution of detector efficiency for the individual channels is most homogenous. In this sense, the data corrections after acquisition are minimal and the collected scattering data are most reliable.

The Dutch company Amsterdam Scientific Instruments produces silicon-based detectors with extremely high counting rates (many MHz) and spatial resolution (55 µm). Each detector channel is equipped with individual electronics, which serves these high demands. For counting neutrons, there must be a boron-based converter. The drawback of this technique is the gamma sensitivity, and such events must be suppressed by software. The practical signal to noise ratio must be explored experimentally. However, this technique is favorable for the central 'beam-stop' detector, which determines the wavelength dependent transmission and center position. Furthermore, the VSANS and SESANS options require such a technique as well. So, this technique will be explored within the SKADI project.

The company DENEX is experienced in gas detectors, and will extend their expertise to boron-based converter detectors with gas tubes. The array of tubes will be two-dimensional (in neutron flight direction and perpendicular) with the tubes being vertical. By analyzing the decay of intensities in the flight direction, the neutron wavelength might be analyzed. For the inelastic scattering of water (for example) the separation of neutron wavelengths might be beneficial, because the unwanted background can be better subtracted (if this technique works well).

The Forschungszentrum Jülich is experienced in building scintillation-based detectors. Usually, the photomultipliers are relatively large – at least larger than a single detector channel. The scaling of the photomultipliers to smaller sizes and parallel read-outs (and reconstruction) would enable this technique to be used up to several 10 MHz.

For the primary beam detector also nitrogen-based gas detectors might provide a good solution. Here, discussions with FRM-2 (K. Zeitlhack) are ongoing.

Supporting Facilities

Necessary facilities to support scientific operation at SKADI should help primarily in sample preparation, sample environment and additional sample characterization. In order to achieve

these goals standard biological and chemical labs are needed. In this context, also a chemical/biological deuteration facility is highly desirable as to allow for preparation of deuterated samples on site. Also a wide range of ovens, freezers and sample storage facilities will be needed. Sample environment labs should be able to provide and support sample holders for various sample geometries and physical conditions, including temperature, pressure, mechanical strain and electric and magnetic fields. Here it is important to stress there should be a close connection to the planned Data Management and Software Center to be able to control the various sample environments in the measurement software and also to store the resulting metadata along with the neutron measurement data. For sample characterization a wide range of different equipment is conceivable, from light-scattering and SAXS setups to rheometers and UV-Vis or IR-Spectrometers to DSC, SQUID or x-ray diffractometers.

Costing

1.4 The details of the costing have been divided to the following segments:

Integrated Design: The effort from the Lead Scientist and engineer

Systems Integration Systems: engineering activities to ensure compatibility between components and compliance with ESS standards.

Detectors and Data Acquisition: Detector systems complete with all electronics. Different realizations are discussed in parallel – the final costs will nonetheless be approx. constant.

Optical Components: The beam delivery system including the bender, guide, the guide housing, alignment system, collimation slits and collimation housing, and the He3 analyzer.

Choppers: The chopper systems for bandwidth selection and frame overlap suppression

Detector Vessel: The vacuum vessel for the detectors, including windows.

Sample Environment: The necessary hexapod and translation stages for mounting sample environment.

Shielding: The shielding solutions required for radiation protection and background reduction, including shutter systems.

Instrument Specific Support Equipment: cabins, mezzanines, raised floor areas. As no definite floor plan exists at the moment, the estimate here is based on information from SNS and ISIS.

	Phase 1 (Designing and Planning) 18 months			Phase 2 (Final Design) 18 months			Phase 3 (Procurement and Installation) 24 months			Phase 4 (Beam Testing and Comissioning) 12 months			Total			
	Hardware (k€)	Staff (k€)	Staff (Months)	Hardware (k€)	Staff (k€)	Staff (Months)	Hardware (k€)	Staff (k€)	Staff (Months)	Hardware (k€)	Staff (k€)	Staff (Months)	Hardware (k€)	Staff (k€)	Staff (Months)	Staff (years)
Integrated Design	0	360	36	0	360	36	0	480	48	0	160	16	0	1360	136	11.33
Systems Integration	10	90	9	450	90	9	10	120	12	10	30	3	480	330	33	2.75
Detectors and Data Acquisition	1000	180	18	3000	180	18	100	120	12	20	30	3	4120	510	51	4.25
Optical Components	50	25	2.5	900	85	8.5	110	240	24	30	40	4	1090	390	39	3.25
Choppers	200	25	2.5	1000	25	2.5	10	40	4	10	10	1	1220	100	10	0.83
Detector Vessel	60	50	5	500	50	5	10	160	16	10	40	4	580	300	30	2.50
Sample Environment	0	50	5	700	50	5	10	40	4	10	10	1	720	150	15	1.25
Shielding	100	50	5	1700	50	5	10	160	16	10	40	4	1820	300	30	2.50
Instrument Specific Support Equipment	0	0	0	0	25	2.5	100	100	10	20	20	2	120	145	14.5	1.21
Instrument Infrastructure	0	25	2.5	0	25	2.5	400	40	4	10	10	1	410	100	10	0.83
Total	1420	855	85.5	8250	940	94	760	1500	150	130	390	39	10560	3685	368.5	30.71
Grand Total (no VAT)	14245															

Table 1.1: Detailed costing plan for SKADI over 4 phases.

Abbreviation	Explanation of abbreviation
SKADI	**Small K Advanced Diffraction Instrument**
SANS	**Small Angle Neutron Scattering**
VSANS	**Very Small Angle Neutron Scattering**
SESANS	**Spin Echo Small Angle Neutron Scattering**
SAXS	**Small Angle X-ray Scattering**
SLS	**Static Light Scattering**
DLS	**Dynamic Light Scattering**
TOF	**Time-of-Flight**

PROPOSAL HISTORY

New proposal:	yes
Resubmission:	no

LITERATURE

1. Clarkson, C. R.; Solano, N.; Bustin, R. M.; Bustin, A. M. M.; Chalmers, G. R. L.; He, L.; Melnichenko, Y. B.; Radlinski, A. P.; Blach, T. P., *Fuel* **103**, 606-616.(2013)

2. Hoagie, M.; Amorer, G.; Wang, X.; Economides, M. In *The Role of Underground Storage in Large Natural Gas Production Operation*, IPTC 2013: International Petroleum Technology Conference, 2013; 2013.

3. Specht, M.; Baumgart, F.; Feigl, B.; Frick, V.; Stürmer, B.; Zuberbühler, U.; Sterner, M.; Waldstein, G., Storing Bioenergy and Renewable Electricity in the Natural Gas Grid. *Renewable Energy Research Association, Topics 2009* 2009.

4. Orimo, S. I.; Nakamori, Y.; Eliseo, J. R.; Zuttel, A.; Jensen, C. M., *Chem. Rev.* **107**, 4111-4132.(2007)

5. Melnichenko, Y. B.; Radlinski, A. P.; Mastalerz, M.; Cheng, G.; Rupp, J., *Int. J. Coal Geol.* **77**, 69-79.(2009)

6. Iturbe, R.; Flores, C.; Chavez, C.; Bautista, G.; Torres, L. G., *Journal of Soils and Sediments* **4**, 115-122.(2004)

7. Takahashi, R.; Sato, T.; Terao, K.; Qiu, X. P.; Winnik, F. M., *Macromolecules* **45**, 6111-6119.(2012)

8. Dvorak, J.; Sklenicka, V.; Betekhtin, V. I.; Kadomtsev, A. G.; Kral, P.; Kvapilova, M.; Svoboda, M., *Mater. Sci. Eng. A-Struct. Mater. Prop. Microstruct. Process.* **584**, 103-113.(2013)

9. Takemura, T.; Oda, M.; Kirai, H.; Golshani, A., *Int. J. Rock Mech. Min. Sci.* **53**, 76-85.(2012)

10. Blanchard, A.; Graham, R. S.; Heinrich, M.; Pyckhout-Hintzen, W.; Richter, D.; Likhtman, A. E.; McLeish, T. C. B.; Read, D. J.; Straube, E.; Kohlbrecher, J., *Phys. Rev. Lett.* **95**, 4.(2005)

11. Botti, A.; Pyckhout-Hintzen, W.; Richter, D.; Urban, V.; Straube, E., *J. Chem. Phys.* **124**, 5.(2006)

12. Eskildsen, M. R.; Forgan, E. M.; Kawano-Furukawa, H., *Rep. Prog. Phys.* **74**, 13.(2011)

13. Huxley, A.; Rodiere, P.; Paul, D. M.; van Dijk, N.; Cubitt, R.; Flouquet, J., *Nature* **406**, 160-164.(2000)

14. Kerscher, M.; Busch, P.; Mattauch, S.; Frielinghaus, H.; Richter, D.; Belushkin, M.; Gompper, G., *Phys. Rev. E* **83**, 4.(2011)

15. Frielinghaus, H.; Holderer, O.; Lipfert, F.; Monkenbusch, M.; Arend, N.; Richter, D., *Nucl. Instrum. Methods Phys. Res. Sect. A-Accel. Spectrom. Dect. Assoc. Equip.* **686**, 71-74.(2012)

16. Tsakiroglou, C. D.; Aggelopoulos, C. A.; Tzovolou, D. N.; Theodoropoulou, M. A.; Avraam, D. G., *Int. J. Multiph. Flow* **55**, 11-23.(2013)

17. Liang, J. Y.; Chang, S. Q.; Feng, N., *J. Appl. Polym. Sci.* **130**, 510-515.(2013)

18. Allen, A. J.; Thomas, J. J.; Jennings, H. M., *Nat. Mater.* **6**, 311-316.(2007)

19. Navarre-Sitchler, A. K.; Cole, D. R.; Rother, G.; Jin, L. X.; Buss, H. L.; Brantley, S. L., *Geochim. Cosmochim. Acta* **109**, 400-413.(2013)

20. Qiu, H. B.; Cambridge, G.; Winnik, M. A.; Manners, I., *Journal of the American Chemical Society* **135**, 12180-12183.(2013)

21. Chen, Y. C.; Xie, R.; Chu, L. Y., *J. Membr. Sci.* **442**, 206-215.(2013)

22. Cass, P.; Knower, W.; Hinton, T.; Shi, S. N.; Grusche, F.; Tizard, M.; Gunatillake, P., *Acta Biomater.* **9**, 8299-8307.(2013)

23. Van Dyk, A.; Nakatani, A., *J. Coat. Technol. Res.* **10**, 297-303.(2013)

24. Zinn, T.; Willner, L.; Lund, R.; Pipich, V.; Richter, D., *Soft Matter* **8**, 623-626.(2012)

25. Jackson, A. J.; McGillivray, D. J., *Chem. Commun.* **47**, 487-489.(2011)

26. Helgeson, M. E.; Moran, S. E.; An, H. Z.; Doyle, P. S., *Nat. Mater.* **11**, 344-352.(2012)

27. Chu, D. S. H.; Schellinger, J. G.; Bocek, M. J.; Johnson, R. N.; Pun, S. H., *Biomaterials* **34**, 9632-9637.(2013)

28. Yan, L.; Li, G. X.; Zhang, S.; Sun, F.; Huang, X. J.; Zhang, Q.; Dai, L. M.; Lu, F.; Liu, Y., *Chin. Sci. Bull.* **58**, 2347-2352.(2013)

29. Li, J.; Fan, C. H.; Pei, H.; Shi, J. Y.; Huang, Q., *Adv. Mater.* **25**, 4386-4396.(2013)

30. Radulescu, A.; Fetters, L. J.; Richter, D.; Springer-Verlag, B., Polymer-Driven Wax Crystal Control Using Partially Crystalline Polymeric Materials. In *Wax Crystal Control: Nanocomposites, Stimuli-Responsive Polymers*, Springer-Verlag Berlin: Berlin, 2008; Vol. 210, pp 1-100.

31. Minton, A. P., *Biopolymers* **99**, 239-244.(2013)

32. Castelletto, V.; Hamley, I. W.; Whitehouse, C.; Matts, P. J.; Osborne, R.; Baker, E. S., *Langmuir* **29**, 9149-9155.(2013)

33. Sorensen, H.; Pedersen, J. S.; Mortensen, K.; Ipsen, R., *Int. Dairy J.* **33**, 1-9.(2013)

34. Adams, J.; Allgaier, J.; Frank, C. Mixture for Emulsion for Use as Cleaner for Use in Printing Industry, Cleaning Printing Cylinder, Shaft and Surfaces of Printers, Colors and Lacquers, Salty and Oily Residue, and for Cosmetic Products and Food, Comprises Two Components. WO2008132202-A2; WO2008132202-A3; EP2152843-A2; US2010144898-A1; JP2010525132-W, WO2008132202-A2 06 Nov 2008 C11D-003/37 200925.

35. Klemmer, H.; Strey, R., In University Cologne.

36. Costeux, S.; Zhu, L. B., *Polymer* **54**, 2785-2795.(2013)

37. Fert, A.; Cros, V.; Sampaio, J., *Nat. Nanotechnol.* **8**, 152-156.(2013)

38. Milde, P.; Kohler, D.; Seidel, J.; Eng, L. M.; Bauer, A.; Chacon, A.; Kindervater, J.; Muhlbauer, S.; Pfleiderer, C.; Buhrandt, S.; Schutte, C.; Rosch, A., *Science* **340**, 1076-1080.(2013)

39. Romming, N.; Hanneken, C.; Menzel, M.; Bickel, J. E.; Wolter, B.; von Bergmann, K.; Kubetzka, A.; Wiesendanger, R., *Science* **341**, 636-639.(2013)

40. Seki, S.; Yu, X. Z.; Ishiwata, S.; Tokura, Y., *Science* **336**, 198-201.(2012)

41. Mühlbauer, S.; Binz, B.; Jonietz, F.; Pfleiderer, C.; Rosch, A.; Neubauer, A.; Georgii, R.; Böni, P., *Science* **323**, 915-919.(2009)

42. Thomson, T.; Toney, M. F.; Raoux, S.; Lee, S. L.; Sun, S.; Murray, C. B.; Terris, B. D., *J. Appl. Phys.* **96**, 1197-1201.(2004)

43. Zhao, Z. H.; Zhou, Z. J.; Bao, J. F.; Wang, Z. Y.; Hu, J.; Chi, X. Q.; Ni, K. Y.; Wang, R. F.; Chen, X. Y.; Chen, Z.; Gao, J. H., *Nat. Commun.* **4**, 7.(2013)

44. Lee, J.-H.; Jang, J.-t.; Choi, J.-s.; Moon, S. H.; Noh, S.-h.; Kim, J.-w.; Kim, J.-G.; Kim, I.-S.; Park, K. I.; Cheon, J., *Nat Nano* **6**, 418-422.(2011)

45. Etoc, F.; Lisse, D.; Bellaiche, Y.; Piehler, J.; Coppey, M.; Dahan, M., *Nat. Nanotechnol.* **8**, 193-198.(2013)

46. Honecker, D.; Michels, A., *Phys. Rev. B* **87**, 10.(2013)

47. Thompson, R. B.; Ginzburg, V. V.; Matsen, M. W.; Balazs, A. C., *Science* **292**, 2469-2472.(2001)

48. Xia, X.; Metwalli, E.; Ruderer, M. A.; Korstgens, V.; Busch, P.; Boni, P.; Muller-Buschbaum, P., *J. Phys.-Condes. Matter* **23**, 9.(2011)

49. Disch, S.; Wetterskog, E.; Hermann, R. P.; Wiedenmann, A.; Vainio, U.; Salazar-Alvarez, G.; Bergstrom, L.; Bruckel, T., *New J. Phys.* **14**, 11.(2012)

50. Krycka, K. L.; Booth, R. A.; Hogg, C. R.; Ijiri, Y.; Borchers, J. A.; Chen, W. C.; Watson, S. M.; Laver, M.; Gentile, T. R.; Dedon, L. R.; Harris, S.; Rhyne, J. J.; Majetich, S. A., *Phys. Rev. Lett.* **104**, 4.(2010)

51. Mikhail, V. A.; Viktor, L. A., *Physics-Uspekhi* **53**, 971.(2010)

52. Wiedenmann, A.; Keiderling, U.; Habicht, K.; Russina, M.; Gahler, R., *Phys. Rev. Lett.* **97**, 4.(2006)

53. Theis-Bröhl, K.; Mishra, D.; Toperverg, B. P.; Zabel, H.; Vogel, B.; Regtmeier, A.; Hütten, A., *J. Appl. Phys.* **110**, 5.(2011)

54. Ryukhtin, V.; Saruhan, B.; Ochrombel, R.; Noirez, L.; Wiedenmann, A.; Iop, *5th European Conference on Neutron Scattering* **340**, 7.(2012)

55. Lippmann, T.; Beckmann, F. Harwi Ii.

56. The Engineering Materials Diffractometer at Sns.

57. Chaboussant, G.; Desert, S.; Brulet, A., *Eur. Phys. J.-Spec. Top.* **213**, 313-325.(2012)

58. Bouwman, W. G.; Duif, C. P.; Plomp, J.; Wiedenmann, A.; Gahler, R., *Physica B* **406**, 2357-2360.(2011)

Appendix

List of Letters of Interest

Name	Area	Country
Marie-Sousai Appavou	Biology	Germany
Arantxa Arbe	Polymers	Spain
Havazelet Bianco-Peled	Polymers	Israel
Ralf Biehl	Biology	Germany
Amélie Banc	Materials	France
Laurent Bouteiller	Polymers	France
Wim G. Bouwman	Food Science	Netherlands
Stéphanie Cassel	Materials	France
Jean-Paul Chapel	Polymers	France
Yachin Cohen	Polymers	Israel
Olivier Colombani	Polymers	France
Fabrice Cousin	Polymers	France
Christophe Dejugnat	Chemistry	France
Olivier Diat	Polymers	France
Sabrina Disch	Materials	France
J-Paul Douliez	Biology	France
Cécile Dreiss	Polymers	UK
Emmanuelle Dubois	Materials	France
S.U. Egelhaaf	Chemistry	Germany
Zhengdong Fu	Physics	Germany
Jacek Gapinski	Biology	Poland
Gérard Gebel	Materials	France
Ralph Gilles	Materials	Germany
Valentin Gogonea	Biology	USA
Ian W. Hamley	Biology	UK
Thomas Hellweg	Materials	Germany

Janosch Henning	Biology	Germany
Marianne Impéror-Clerc	Materials	France
Kell Mortensen	Polymers	Denmark
Helge Klemmer	Chemistry	Germany
Margarita Krutyeva	Biology	Germany
André Kusmin	Chemistry	Germany
Clémence Le Coeur	Polymers	France
Pavlik Lettinga	Physics	Belgium
Christian Ligoure	Physics	France
Frederik Lipfert	Materials	Germany
Sébastien Livi	Polymers	France
Reidar Lund	Chemistry	Norway
Robert Luxenhofer	Polymers	Germany
Paula Malo de Molina	Materials	USA
Manuel Maréchal	Polymers	France
Martine Philipp	Polymers	Germany
Andreas Michels	Physics	Luxembourg
Francesco Stellacci	Materials	Italy
Angel Muñoz Castellanos	Energy	Spain
Frédéric Nallet	Chemistry	France
Georg Pabst	Biology	Austria
Luigi Paduano	Chemistry	Italy
Aristeidis Papagiannopoulos	Polymers	Greece
Adam Patkowski	Polymers	Poland
Alain Pautrat	Materials	France
Michel Rawiso	Polymers	France
Manuchar Rawiso	Polymers	France
FrantiSek Rypacek	Chemistry	Czech
Saha Debasish	Biology	France
Olivier Sandre	Polymers	France
Frank Schreiber	Biology	Germany
Dietmar Schwahn	Biology	Germany
Simona Sennato	Materials	Italy
Olivier Spalla	Biology	France
Jörg Stellbrink	Polymers	Germany
Bernd Stühn	Polymers	Germany
Regine von Klitzing	Polymers	Germany
Yue Zhao	Materials	Japan
Mehdi Zeghal	Physics	France
Bo Zhang	Biology	Germany
Fajun Zhang	Biology	Germany
Tobias Schrader	Biology	Germany
Wim Pyckhout-Hintzen	Materials	Germany